Hydrogen-rich gas production by continuous pyrolysis and in-line catalytic reforming of pine wood waste and HDPE mixtures

Aitor Arregi, Maider Amutio, Gartzen Lopez*, Maite Artetxe, Jon Alvarez, Javier Bilbao and Martin Olazar

Department of Chemical Engineering, University of the Basque Country UPV/EHU, P.O. Box 644 - E48080 Bilbao (Spain). gartzen.lopez@ehu.es

Abstract

The continuous pyrolysis-catalytic steam reforming of different mixtures of biomass and high density polyethylene (25, 50 and 75 wt % HDPE) has been carried out in a two-step reaction system, provided with a conical spouted bed reactor (CSBR) and fluidized bed. The influence of HDPE co-feeding on the conversion, reforming products yields and composition and catalyst deactivation has been studied at a reforming temperature of 700 ºC, with 16.7 g_{cat} min $g_{feeding}^{-1}$ and steam/(biomass+HDPE) mass ratio of 4, comparing the results with those obtained by feeding pure biomass and HDPE. The co-feeding of plastics enhances the production of hydrogen, which increases from 10.9 g of H_2 per 100 g of biomass to 37.3 g of H_2 per 100 g of HDPE fed. Catalyst deactivation by coke is attenuated when HDPE is co-fed due to the lower content of oxygenated compounds in the reaction environment. The higher yield of hydrogen achieved with this two-step (pyrolysis-reforming) strategy, its flexibility to jointly valorise biomass and plastic mixtures and the lower temperatures required in relation to gasification, makes this process promising to produce H_2 from renewable raw materials and wastes.

Keywords: hydrogen; pyrolysis; reforming; biomass; waste plastics; conical spouted bed, catalyst deactivation

1. Introduction

The environmental awareness associated with the use of traditional resources (natural gas, petroleum and coal) gives way to the development of new routes for sustainable hydrogen production, whose demand is growing due to its interest as energy carrier and reactant in refinery hydroprocessing units [1]. In this scenario, biomass can play an important role as an alternative feedstock, given that is a CO_2 neutral renewable source and chemicals or fuels produced from it are considered sustainable [2].

Amongst the different thermochemical routes, direct steam gasification [3-6] and the indirect route of bio-oil reforming [7-10] are the most studied routes for hydrogen production from biomass. Nevertheless, the gasification process is directed to produce syngas and the tar formation is an issue for its industrial applications [11,12]. On the other hand, the indirect route of bio-oil reforming has several problems related to bio-oil properties and its vaporization and re-polymerization [13,14]. Therefore, the two-step pyrolysis-catalytic steam reforming process, in which is not necessary to condensate and re-vaporized the bio-oil, is gaining attention last years [15-19]. This process, in which each step is carried out in different reactors, involves some advantages in relation to one-step pyrolysis process with a reforming catalyst in-situ. On the one hand, the temperature of each step can be optimized in order to maximize the production of hydrogen [20] and on the other hand, the catalyst is more effective for volatiles transformation and the process is more versatile in order to establish the desired catalyst/feeding ratio. Therefore, a more homogeneous product stream will be obtained, due to the higher efficiency of the catalyst in order to attenuate secondary reactions.

48 Nevertheless, the low content of hydrogen and high content of oxygen of the biomass
49 feedstock is a drawback to obtain high production of hydrogen. Moreover, the catalyst
50 has a considerable deactivation by coke [17]. In this work, the improvement of H_2
51 production and the attenuation of catalyst deactivation by the valorisation of biomass
52 and HDPE mixtures has been studied.

53 The improvement on hydrogen production has been reported by several authors in the
54 co-gasification of biomass and HDPE mixtures [21-24]. The co-feeding solves the
55 seasonal limitations of biomass availability and contributes to attenuate the
56 environmental problems associated to the waste plastics management. Even though the
57 pyrolysis is considered a suitable route for the valorisation of waste plastics on a large
58 scale, and particularly for polyolefins [25-27], the studies concerning pyrolysis and in-
59 line catalytic steam reforming of biomass and plastic mixtures are very scarce. Alvarez
60 et al. [20] studied the co-feeding of polypropylene in pyrolysis-reforming of biomass in
61 batch laboratory scale reactor, obtaining higher gas yield and higher hydrogen
62 production in relation to feeding pure biomass. In the same experimental unit Kumagai
63 et al. [28] tested a Ni-Mg-Al-Ca catalyst synthesized by a co-precipitation method for
64 pyrolysis-reforming of a biomass/polypropylene mixture, obtaining a maximum
65 hydrogen production of 6.0 g of H_2 per 100 g of feeding when the catalyst was calcined
66 at low temperatures, 500 ºC.

67 The aim of this work is to increase the production of hydrogen by plastics co-feeding,
68 using a continuous two-step process (Figure 1). The equipment combines the excellent
69 performance of the conical spouted bed reactor (CSBR) for the pyrolysis of biomass
70 [29] and plastics [30] with the suitability of the fluidized bed reactor for the steam
71 reforming process [31,32]. The cyclic vigorous movement of the sawdust and sand
72 particles coated with melted plastic in the CSBR minimizes the segregation problems

and avoids the defluidization of the bed. On the other hand, the fluidized bed catalytic reactor allows controlling the temperature of the endothermic reforming reaction and delays the blocking of the bed by coke formation. This two step configuration has been described in previous papers for the pyrolysis-catalytic steam reforming of biomass [17] and plastics [33], in which the good performance of the process without operational problems and high hydrogen yields were reported.

Figure 1 (falta este haremos un esquema del proceso)

2. Materials and Methods

2.1. Materials

Pine sawdust *(pinus insignis)* waste has been crushed, ground and sieved to a particle size between 1 and 2 mm, which is a suitable particle diameter in order to guarantee the good performance of the solid feeding system, and dried at room temperature to a moisture content below 10 wt %. The high density polyethylene (HDPE) was provided by Dow Chemical (Tarragona, Spain) in the form of chippings (4 mm), with the following properties: average molecular weight, 46.2 kg mol^{-1}; polydispersity, 2.89 and density, 940 kg m^{-3}. The higher heating value (HHV) of both feedstocks has been measured in a Parr 1356 isoperibolic bomb calorimetry. Moreover, the ultimate and proximate analyses have been determined in a LECO CHNS-932 elemental analyzer and in a TGA Q5000IR thermogravimetric analyzer, respectively and the results of the characterization of biomass and HDPE used in this study are summarized in Table 1.

Table 1. Characterization of the biomass and HDPE used.

Ultimate analysis (wt %)	**Biomass**	**HDPE**
Carbon	49.33	85.71

Hydrogen	6.06	14.29
Nitrogen	0.04	0
Oxygen	44.57	0
Proximate analysis (wt %)		
Volatile matter	73.4	99.7
Fixed carbon	16.7	0.3
Ash	0.5	-
Moisture	9.4	-
HHV (MJ kg^{-1})	19.8	43.1

A commercial Ni reforming catalyst (G90-LDP) provided by Süd Chemie (Germany) has been used for the reforming step. The original catalyst (in the form of perforated rings 19 x 16 mm) has been ground and sieved between 0.4-0.8 mm, which is the suitable particle size in order to guarantee the fluid dynamic conditions of the fluidized bed. The metal content (provided by the supplier) and physical properties of the catalyst are summarized in Table 2. The adsorption-desorption isotherm of the catalyst has been measured by N_2 adsorption-desorption (Micromeritics ASAP 2010). As observed, the catalyst shows low BET surface area and low porosity.

Table 2. Metal content and physical properties of the catalyst.

Catalyst	**NiO content (wt %)**	**S_{BET} (m^2 g^{-1})**	**V_{porous} (cm^3 g^{-1})**	**d_{porous} (Å)**
G90-LDP	14	19	0.04	122

Moreover, the catalyst has been reduced in-situ in order to ensure its activity. The reduction has been conducted for 4 h under 10 vol % H_2 at 710 ºC according to the results obtained by temperature programmed reduction. Both the adsorption-desorption isotherm and the TPR profile of this catalyst can be found elsewhere [34,35].

2.2. Equipment and reactors

Figure 2 shows the scheme of the experimental equipment. The plant is provided with two reactors in-line: (i) a CSBR for pyrolysis step and (ii) a fluidized bed reactor for the reforming step of pyrolysis volatiles.

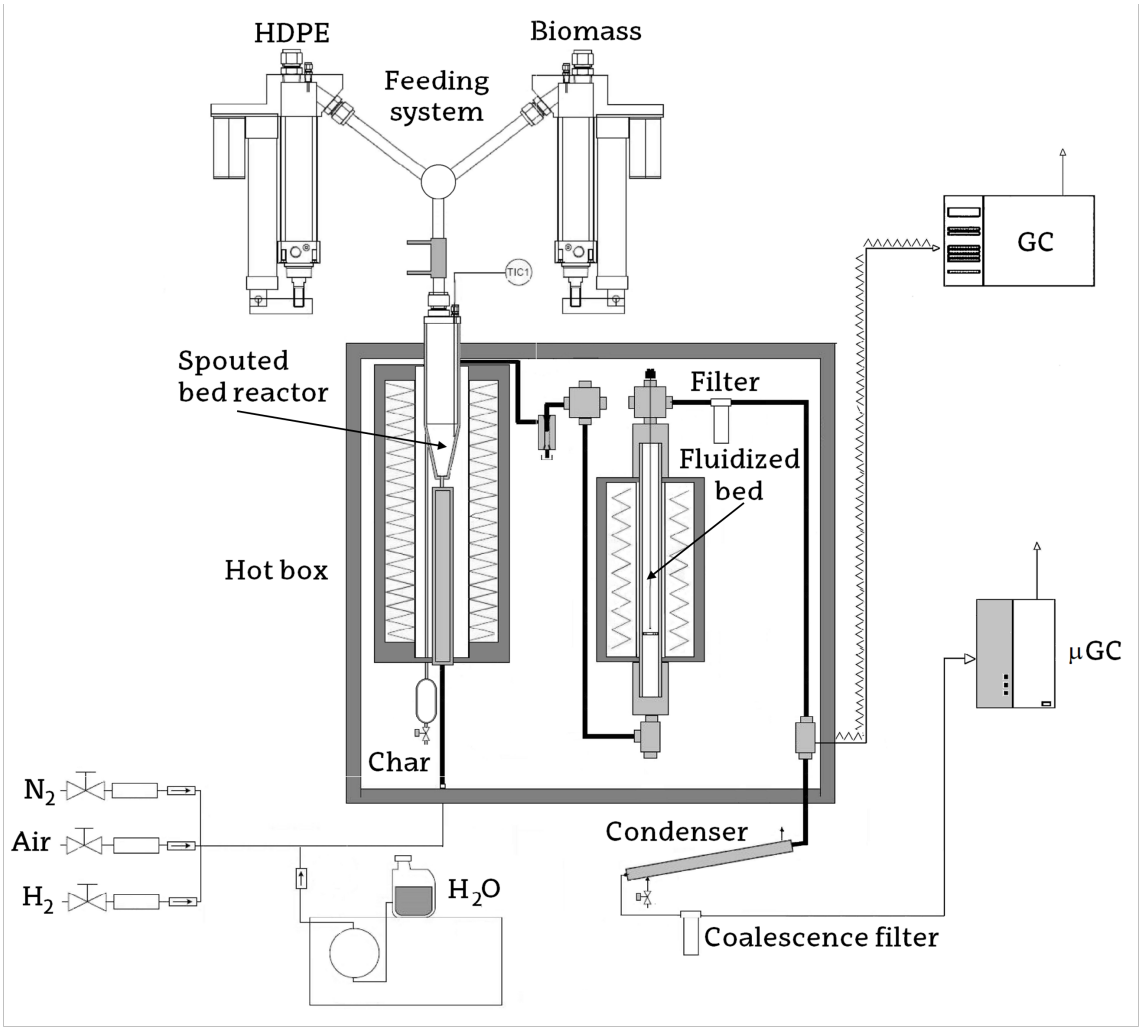

Figure 2. Scheme of the bench scale unit.

The plant is provided with two independent feeders for biomass and HDPE as segregation problems took place when both materials were mixed in a single unit. Each feeder consists of a vessel equipped with a vertical shaft connected to a piston placed below the material bed. The material is fed into the reactor by raising the piston at the same time as the whole system is vibrated by an electric engine. The pipe that connects

120 the feeders with the reactor is cooled with tap water. Moreover, a very small nitrogen
121 flow is introduced into the vessel, which avoids the condensation of steam in the
122 feeding vessel.

123 A pump (Gilson 307) has been used in order to feed the water into the pyrolysis reactor,
124 which has been previously vaporized by an electric cartridge placed inside the forced
125 convection oven. Nitrogen, air or hydrogen can also be introduced to the CSBR reactor
126 and their flows are controlled by mass flow controllers, which allow feeding up to 20 L
127 min^{-1} of nitrogen and air, and up to 5 L min^{-1} of hydrogen. The temperature of the steam
128 and the gases is increased up to reaction conditions in a gas preheater located in the
129 lower section of the reactor, which is filled with stainless steel pipes that increase the
130 surface area for heat transfer.

131 The pyrolysis step has been carried out in a CSBR. This reactor has been successfully
132 used in the pyrolysis and gasification of different waste materials, such as biomass
133 [5,36], plastics [37,38] and tyres [39,40]. The detailed design and main dimensions of
134 the CSBR can be found elsewhere [17,33]. The temperature of the reactor is controlled
135 by two thermocouples located inside the reactor, one in the bed annulus and the other
136 one close to the wall. Prior entering the reforming reactor the product stream is cleaned
137 by a high-efficiency cyclone, for retaining the fine sand and char particles entrained
138 from the CSBR.

139 In order to avoid the blocking of the flow due to the coke deposition, which has been
140 observed in a fixed bed reactor [34], the reforming step has been carried out in a
141 fluidized bed reactor, whose dimensions are 38.1 mm of diameter and 440 mm of
142 length. The temperature of the fluidized bed reactor is controlled by a thermocouple
143 placed inside the catalyst bed. The volatiles from fluidized bed reactor circulate through

a sintered steel filter (5 μm) to retain catalyst fines elutriated from the fluidized bed, with this amount being bellow 5% of the catalyst used in the experiments performed. All the interconnection pipes, cyclone, filter and both reactors are located inside an oven kept at 270 ºC, which ensures that the steam and products are not condensed in the connections between the reactors.

Finally, the condensation system of the plant ensures total condensation and retention of non-reacted steam and biomass and HDPE derived products, which consists of a condenser and a coalescence filter.

2.3. Experimental conditions

The fluid dynamic requirements of the two reactors in-line with a common gas flow have conditioned the steam flow and the particle size of the sand in the CSBR and the particle size of both catalyst and sand in the fluidized bed reactor. Thus, 3 mL min^{-1} of water flow has been established, which corresponds to a steam flow of 3.73 NL min^{-1}, and the bed consists of 50 g of sand in the pyrolysis step, with particle size being between 0.3-0.35 mm. The runs have been carried out in continuous regime by feeding 0.75 g min^{-1} of biomass and HDPE mixtures. Moreover, the pyrolysis step has been carried out at 500 ºC, which has been proved in previous studies to be a suitable temperature for biomass [29] and HDPE pyrolysis [30] in a CSBR.

In the same way, after fluid dynamic tests, a bed of 25 g of catalyst and sand mixture has been established for the fluidized bed reactor, with particle size being between 0.4-0.8 mm for the catalyst and 0.3-0.35 mm for the sand, in order to work with a relative velocity 3 or 4 times higher than minimum fluidization velocity. These conditions guarantee the complete fluidization of the bed, even when the coke content of the catalyst is high.

The effect of feeding different HDPE/biomass mass ratios in the pyrolysis-reforming process has been studied. Thus, HDPE/biomass mixtures of 25/75, 50/50 and 75/25 wt % have been tested and the results have been compared with those of pure biomass and plastic feeds. The temperature of the reforming step was 700 ºC, given that is the minimum temperature needed for the complete conversion of volatiles from HDPE pyrolysis [33]. The other operating conditions of the process are the following: 16.7 g_{cat} min $g_{feeding}^{-1}$ (corresponding to 12.5 g of catalyst) and steam/(biomass+HDPE) mass ratio of 4. The runs have been repeated several times (at least 3) under the same conditions in order to guarantee reproducibility of the results.

2.4. Product analysis

The volatile products of the reforming step have been analysed on-line by means of a GC Agilent 6890 provided with a HP-Pona column and a flame ionization detector (FID). The sample has been transferred from the reactor to the GC by means of a thermostated line at 280 ºC, in order to avoid the condensation of heavy compounds. Moreover, the non-condensable gases have been analyzed on-line in a micro GC (Varian 4900) once the gases were completely free of steam and non-reacted liquid products.

The coke content deposited on the reforming catalyst has been determined at the end of continuous experiments by temperature programmed oxidation (TPO) in a thermobalance TGA Q5000 (TA Instruments), which was connected on-line to a mass spectrometer Thermostar (Balzers Instruments), given that the Ni of the catalyst is oxidized together with the carbonaceous coke, and accordingly, the carbon dioxide formation must be monitored to determine TPO curves. The following procedure has been carried out: (i) signal stabilization with He stream (10 mL min^{-1}) at 100 ºC, (ii)

192 oxidation with air (50 mL min^{-1}) up to 800 ºC with a ramp of 5 ºC min^{-1}, which is
193 maintained for 30 min in order to ensure total coke combustion. In addition, the nature
194 of the coke deposited on the catalyst has been studied by TEM (transmission electron
195 microscopy) images, obtained by means of a Philips CM200.

196 **2.5. Reaction indexes**

197 In order to ease the analysis of the obtained results, the following reaction indexes have
198 been considered: conversion, individual reforming products yields, production of gas,
199 production and stoichiometric yield of H_2 and reacted steam. The conversion has been
200 defined as the ratio between the carbon units in the gaseous product and those fed into
201 the reforming step, taking into account the HDPE/biomass mass ratio of each
202 experiment:

203 $$X = \frac{C_{gas}}{C_{volatiles}} 100 \quad (1)$$

204 It can be pointed out that the carbon contained in the biomass char is not considered for
205 conversion calculation as it is not converted in the reforming step.

206 Moreover, the yield of carbon containing individual compounds (CO, CO_2, CH_4, C_2-C_4
207 fraction, mainly ethylene and ethane) has been based on the volatiles stream from
208 biomass and HDPE mixtures pyrolysis:

209 $$Y_i = \frac{F_i}{F_{volatiles}} 100 \quad (2)$$

210 where F_i and $F_{volatiles}$ are the molar flow rates of product i and pyrolysis volatiles,
211 respectively, both given in carbon units contained.

The hydrogen yield was calculated as a percentage of the maximum allowed by stoichiometry:

$$Y_{H_2} = \frac{F_{H_2}}{F^0_{H_2}} 100 \quad (3)$$

where F_{H2} and F^0_{H2} are the hydrogen molar flow rate obtained in the run and the stoichiometric maximum of the volatiles fed to the reforming reactor, considering the following stoichiometry of the reforming reactions:

Reforming of biomass pyrolysis products:

$$C_nH_mO_k + (2n-k)H_2O \rightarrow nCO_2 + (2n + m/2 - k)H_2 \quad (4)$$

Reforming of HDPE pyrolysis products:

$$C_nH_m + 2nH_2O \rightarrow nCO_2 + (2n + m/2)H_2 \quad (5)$$

The production of gas has been calculated as follows:

$$P_{gas} = \frac{m_g}{m_0} 100 \quad (6)$$

where m_g and m_0 are the mass flows of gas produced and the feeding (HDPE/biomass), respectively.

Equally, the production of H_2 is:

$$P_{H_2} = \frac{m_{H_2}}{m_0} 100 \quad (7)$$

where m_{H2} and m_0 are the mass flows of H_2 and the feeding (HDPE/biomass), respectively.

Finally, the reacted steam (R_{steam}) in the reforming step is calculated based on the hydrogen mass balance, considering the hydrogen content in the volatiles, the water fed into the reaction medium and the H_2 produced.

3. Results

3.1. First step: biomass and HDPE pyrolysis

As pointed out above, the steam required for the reforming step has been introduced in the pyrolysis step, as fluidizing agent in the CSBR. Thus, the pyrolysis step has been conducted under steam environment instead of using an inert gas such as N_2, which is the most commonly used gas in pyrolysis processes. As the pyrolysis step is carried out at relatively low temperatures, a limited difference between the product distributions obtained under steam and nitrogen environment has been observed in previous studies, both in the pyrolysis of biomass [17] and HDPE [33,34]. Similarly, other studies from the literature doesn't show a relevant effect of steam in the pyrolysis of both materials, at least when the pyrolysis was performed at low temperatures [41,42].

Table 3 summarizes the product yields obtained in the pyrolysis reactor for biomass and HDPE. Great differences are observed between the product distributions for both feedings. Thus, the pyrolysis of biomass gives way to three main fractions: gases, bio-oil and char. Under the pyrolysis conditions studied, that is, relatively low temperature and short residence time (fast pyrolysis), the main product obtained is bio-oil (75.3 %). The bio-oil is a complex mixture of several families of oxygenated compounds including acids, aldehydes, alcohols, ketones, phenols, furans and saccharides [26]. Moreover, an important amount of water is produced during biomass pyrolysis due to dehydration reactions and the original moisture content, with its yield being up to 25 %. Due to the mentioned pyrolysis conditions that minimise secondary cracking reactions,

254 the gas yield is 7.3 %, mainly made up of CO and CO_2. Finally, the char yield is of 17.3
255 %, which was removed from the pyrolysis reactor throughout a lateral outlet in order to
256 avoid its accumulation. Although the carbon contained in the char is not reformed in the
257 second step, this product has several applications as active carbon using as sorbent
258 [43,44], catalyst support [45,46], soil amendment [47], etc, and accordingly, its
259 valorisation could contribute to the overall economy of the process.

260 On the other hand, the HDPE pyrolysis doesn´t produce a solid product under fast
261 pyrolysis conditions, which is characteristic of the ability of the CSBR for fast pyrolysis
262 of polyolefins [30,48]. Accordingly, all the products formed are volatiles to be treated in
263 the reforming step. The main products obtained are long chain hydrocarbons composed
264 by diesel fraction (C_{12}-C_{20}) and waxes (C_{21+}), with the total yield being up to 90 %. The
265 yield of gases and gasoline range hydrocarbons is low, 1.5 and 5.6 %, respectively, with
266 the aromatics yield being almost negligible (0.3 %).

267 **Table 3.** Product distribution obtained in the pyrolysis of biomass and HDPE at
268 500 ºC.

Biomass		**HDPE**	
Compound	**Yield (wt %)**	**Compound**	**Yield (wt %)**
Gas	**7.3**	**Gas (C_1-C_4)**	**1.5**
CO	3.38	Alkanes	0.35
CO_2	3.27	Alkenes	1.15
Hydrocarbons (C_1-C_4)	0.68	Butenes	0.57
Bio-oil	**75.3**	**Liquid (C_5-C_{20})**	**31.5**
Acids	2.73	Non-aromatics C_5-C_{11}	5.58
Aldehydes	1.93	Aromatics C_6-C_{11}	0.28
Alcohols	2.00	Aliphatics C_{12}-C_{20}	25.64
Ketones	6.37	Olefins C_{12}-$_{20}$	13.07
Phenols	16.49	Diolefins C_{12}-C_{20}	3.22
Furans	3.32	Paraffins C_{12}-C_{20}	9.35
Saccharides	4.46	**Waxes (C_{21}+)**	**67.0**
Water	25.36	Light waxes (C_{21}-C_{40})	29.5

Char	**17.3**	Heavy waxes (C_{40}+)	37.5

269

270 **3.2. Second step: steam reforming of pyrolysis volatiles**

271 The effect of HDPE co-feeding to biomass pyrolysis-catalytic steam reforming process
272 on conversion and product yields at zero time on stream, and catalyst deactivation has
273 been analysed, with the operating conditions being those described in Section 2.4. In
274 order to analyse the effect of co-feeding on the reaction indexes, the following reactions
275 have been considered:

276 Steam reforming of oxygenates derived from biomass:

277 $$C_nH_mO_k + (n-k)H_2O \rightarrow nCO + (n+m/2-k)H_2 \quad (8)$$

278 Steam reforming of hydrocarbons derived from HDPE:

279 $$C_nH_m + nH_2O \rightarrow nCO + (n+m/2)H_2 \quad (9)$$

280 Water gas shift (WGS): $CO + H_2O \leftrightarrow CO_2 + H_2$ (10)

281 Methane steam reforming: $CH_4 + H_2O \leftrightarrow CO + 3H_2$ (11)

282 Cracking of oxygenated compounds and hydrocarbons (secondary reactions):

283 $$C_nH_mO_k \rightarrow \text{oxygenates} + \text{hydrocarbons} + CH_4 + CO + CO_2 \quad (12)$$

284 $$C_nH_m \rightarrow \text{paraffins} + \text{olefins} \quad (13)$$

285 3.2.1. Results at zero time on stream

286 The experiment performed with different HDPE/biomass mass ratios give way to high
287 conversions (defined in eq. 1) as the space time used is relatively high (16.7 g_{cat} min

288 $g_{feeding}^{-1}$). Thus, conversion is complete when pure biomass is fed into the process and
289 decreases slightly when HDPE is co-fed until 98 % for pure HDPE. The following
290 factors contribute to this slight difference: i) the higher reactivity of oxygenated
291 compounds derived from biomass due to the presence of C=O bonds that ease the
292 formation of carbon oxides in the reforming step [49]; ii) the higher effective space time
293 for biomass feeding. It should be taken into account that the mass of carbon to be
294 reformed when biomass is fed is lower than that with HDPE as biomass contains
295 oxygen in its molecular structure and moreover, a significant fraction of this carbon is
296 retained in the char produced in the pyrolysis step. Therefore, per 100 g of HDPE fed
297 around 85 g of carbon are reformed in the catalytic step, whereas in the case of biomass
298 35 g of carbon are reformed. Consequently, the effective space time (referred to carbon
299 flow rate reaching the reforming reactor) would be around 2.5 times lower for HDPE
300 than that for biomass. Nevertheless, the space time used is enough to guarantee a high
301 conversion for feeds studied.

302 As observed in Figure 3, gas production increases lineally when HDPE is co-fed to the
303 biomass, obtaining a maximum value of 305.0 wt % for pure HDPE. As commented
304 above, this result is a consequence of the higher carbon content of HDPE, which
305 enhances the extent of reforming reactions (eqs. 8 and 9) and provokes an increase of
306 the gas production and reacted steam. In the same line, reacted steam also increases with
307 HDPE content in the feed from 48.9 wt % for pure biomass to 210.9 wt % for pure
308 HDPE.

309 Equally, the co-feeding of HDPE has a great influence on H_2 production, which
310 increases lineally with the HDPE content in the feed. Thus, hydrogen production
311 increases significantly from 10.9 wt % for pure biomass to 37.3 wt % when pure HDPE
312 is fed. This significant difference is directly related with the carbon and hydrogen

313 content of both feedstocks. Given the relation between the results of the reforming step
314 and the composition of the inlet stream to the reactor, the lineal increase of the reaction
315 indexes plotted in Figure 3 shows that there is not a significant synergetic effect of the
316 HDPE co-feeding to the pyrolysis reactor on reforming products composition.
317 Nevertheless, this effect has been observed by other authors, who have verified that the
318 co-pyrolysis of plastics and biomass have a noticeable effect on bio-oil composition
319 [50,51].

320 In order to compare the results in Figure 3 with the literature, it should be pointed out
321 that the pyrolysis and in-line steam reforming of biomass and plastic mixtures is limited
322 to the studies of the research group headed by prof. Williams. Thus, the influence of
323 biomass/polypropylene ratio (feeding between 5 and 20 wt % of PP) has been studied
324 by Alvarez et al. [20] in the batch pyrolysis-reforming process on a Ni/Al_2O_3 catalyst,
325 obtaining a maximum hydrogen production of 5.5 wt %, when 20 wt % of PP was used.
326 Kumagai et al. [28] studied a Ni-Mg-Al-Ca catalyst with different Ca contents and
327 calcination temperatures and the highest hydrogen production of 6.0 wt % was obtained
328 using a calcination temperature of 500 ºC. These results are significantly lower in
329 relation to those obtained in this study, which is a consequence of the continuous mode
330 used in this work. On the other hand, the results reported by other authors for the
331 individual valorization of biomass and plastics by continuous pyrolysis and in-line
332 reforming are in the same range of those obtained in the present study [15,16,52,53].
333 The steam co-gasification of biomass and polyolefins studies reveal the existence of
334 positive and even synergetic effects over the hydrogen and gas production and tar
335 content in the gas product [21-24,54]. However, the hydrogen production obtained in
336 this work is higher than those reported in the steam gasification processes, between 4

337 and 7 wt % for biomass gasification [5,55,56] and in the 6-15 wt % range in the
338 gasification of polyolefins [37,57].

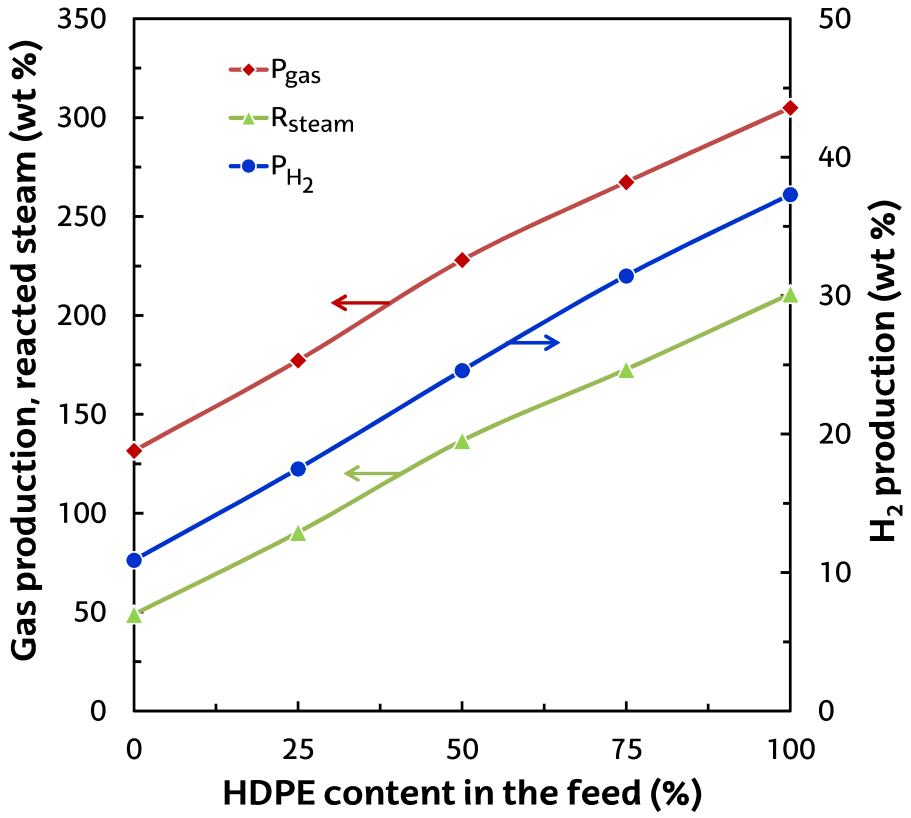

339

340 **Figure 3.** Effect of HDPE co-feeding in the biomass pyrolysis and in-line
341 reforming over gas and hydrogen productions and reacted steam.

342 Figure 4 shows the effect of HDPE content in the feed on individual product yields
343 (graph a) and gas composition (graph b). As it can be observed, there are notable
344 differences in H_2, CO_2 and CO yields distribution. In this way, H_2 and CO_2 yields
345 decrease when HDPE content is increased from 0 to 100 wt %, from 93.2 to 85.7 % and
346 87.2 to 67.4 %, respectively. Nevertheless, CO yield increases from 12.5 to 29.3 %.
347 These results evidence the effect of the higher carbon content of HDPE and therefore,
348 the higher amount of carbon to be reformed. Moreover, as the same space time is used
349 for all experiments, higher yield of CO and lower yield of CO_2 are obtained when

350 HDPE content in the feed is increased, due to the lower extent of WGS reaction (eq.
351 10). It can also be observed that CH_4 and C_2-C_4 yields are very low in all cases studied,
352 although there is a slight increase of these yields when HDPE content is increased from
353 0 to 100 wt %, from 0.2 to 0.8 % for CH_4 and from 0.1 to 0.7 % for C_2-C_4 fraction.

354 It can be pointed out that H_2 concentration increases with HDPE content in the feed
355 until 72 vol % when 75 wt % of HDPE is used (Figure 4b), due to the higher content of
356 hydrogen and lack of oxygen in the plastics composition. Nevertheless, the lower
357 effective space time when HDPE is co-fed gives way to lower CO_2 and higher CO
358 concentrations in the gaseous fraction, which change from 30.2 to 20.9 % and from 4.3
359 to 9.1 %, respectively, in the range of HDPE content studied. The hydrogen
360 concentrations reported by Alvarez et al. [20] in the pyrolysis-reforming of biomass/PP
361 mixtures were below those obtained in the present study, with the maximum value
362 being of 52.1 vol. % for 20 wt % of PP in the feed. The hydrogen concentrations
363 obtained in the steam co-gasification of these feedstocks are also below, in the 40 to 55
364 % range [21,23,58].

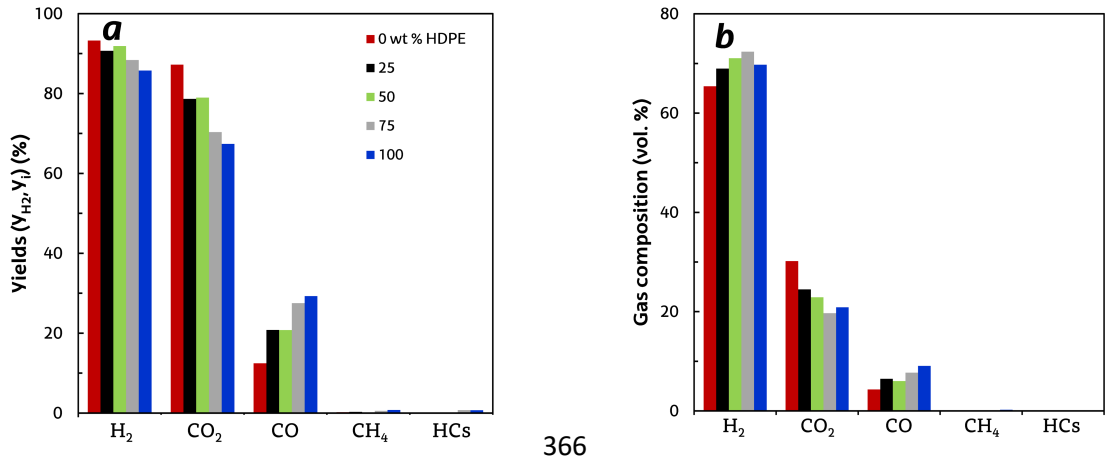

Figure 4. Effect of HDPE co-feeding in the HDPE/biomass mixture fed over the individual products yields (a) and gaseous product concentrations (b), in the pyrolysis and in-line reforming process.

3.2.2. Catalyst deactivation

In order to study the effect of feed composition on the reforming catalyst deactivation, the evolution with time on stream of conversion (Figure 5) and gas composition (Figure 6) in the reforming step has been analyzed. Figure 5 shows that the deactivation behaviour strongly depends on the feed composition. Thus, the conversion in reforming step is below 60 % for pure biomass after 120 min of continuous operation, whereas is higher than 90 % with pure HDPE for the same time on stream. Moreover, it is noteworthy the linear decay of catalyst activity for HDPE, while in the case of biomass, the activity is maintained for the first 60 minutes and follows an acute decreasing trend above 75 minutes.

The initial stable conversion period observed with pure biomass cannot be related to the lower deactivation with this feed, and can be explained due to the space time value in excess with respect to the equilibrium one. Consequently, the higher decrease of the activity observed in Figure 5 for biomass is especially relevant, taking into account the

higher effective space time (around 2.5 times higher) for this feeding. Thus, these results clearly shows that the oxygenated compounds and aromatic rings containing compounds (as phenols) formed in biomass pyrolysis provoked a much faster deactivation than that caused by long chain hydrocarbons from HDPE pyrolysis. In the same line, Czernik et al. [49] remarked that oxygenated compounds have more marked tendency than that of hydrocarbons to form carbonaceous deposits on the catalyst surface and accordingly, provoke a faster catalyst deactivation. In fact, the severe reforming catalyst deactivation has been previously reported by other authors in the reforming of biomass derived oxygenates [59-61].

When different HDPE/biomass mass ratios are used, the conversions evolutions observed are between those of two pure feedings, which confirms that the plastic co-feeding has a notable effect on attenuation of catalyst deactivation.

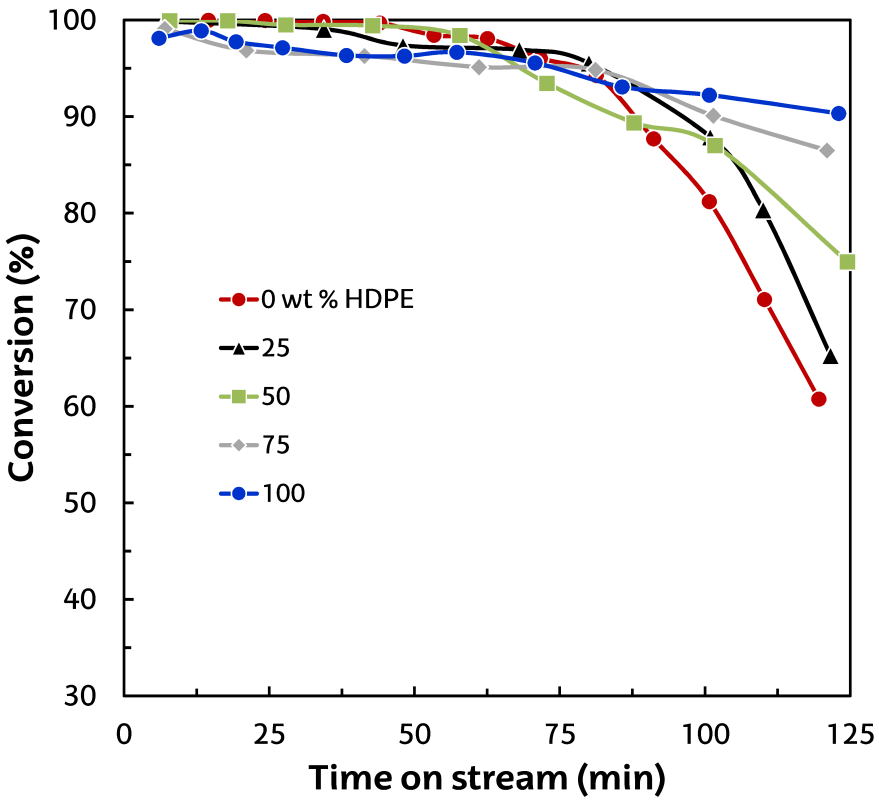

Figure 5. Effect of HDPE content in HDPE/biomass mixture fed over the evolution with time on stream of conversion in the reforming step in pyrolysis and in-line reforming process.

Figure 6 shows the evolution of gas composition with time on stream for three different feedings: pure biomass (a and b), a HDPE/biomass mixture of 50/50 wt % (c), and pure HDPE (d). When pure biomass is used, H_2 concentration decreases from 65 to 55 vol % in 120 min on stream (Figure 6a), whereas it is maintained around 70 vol % when pure HDPE is fed (Figure 6d). Moreover, for pure biomass valorization CO concentration increases from 5 to 16 vol % and the opposite occurs for that of CO_2, which decreases from 30 to 24 vol % after 120 min on stream. This evolution of CO and CO_2 concentrations reveal a significant deactivation of the catalyst towards the WGS reaction (eq. 10). On the other hand, the concentrations of CO and CO_2 remain constant for pure HDPE (Figure 6d) and only change above 75 min on stream for different HDPE/biomass mixtures (Figure 6c). Therefore, when HDPE is co-fed, the deactivation of the WGS reaction is considerably attenuated.

As discussed previously, the concentration of main gaseous products formed by secondary cracking reactions, i.e. CH_4 and C_2-C_4 fraction (ethylene, ethane, propylene and propane, mainly), are very low for different feeds studied due to the initial catalytic activity for both oxygenated compounds and hydrocarbons reforming (eq. (8-9)) and WGS reaction (eq. (10)). However, when the catalyst is deactivated, CH_4 and C_2-C_4 fraction concentrations increase slightly, which is shown in detail in Figure 6b for biomass valorization. A similar although less marked trend can be seen when HDPE is co-fed (results not shown).

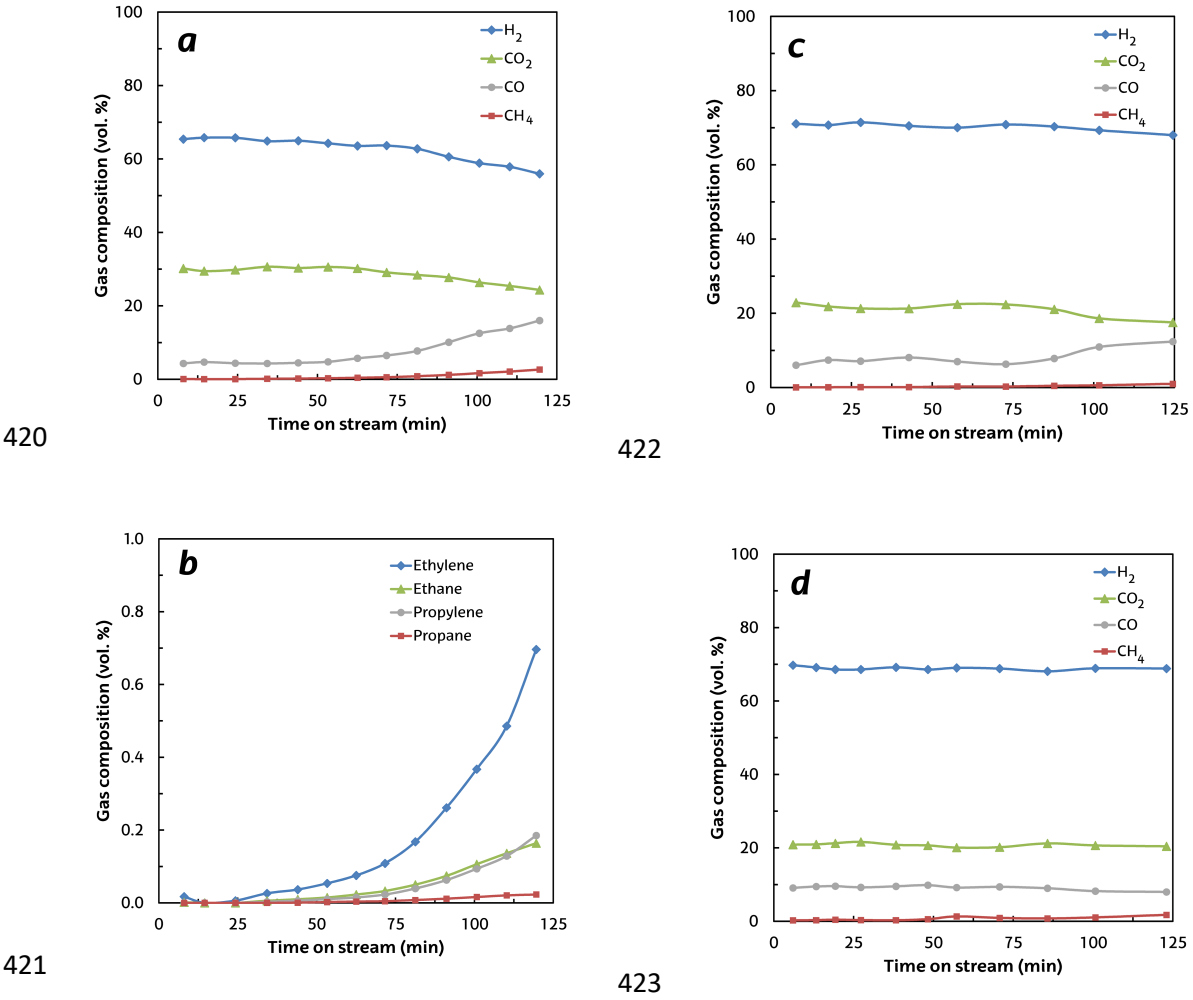

Figure 6. Evolution with time on stream of gas composition in the pyrolysis-reforming of pure biomass (a and b), HDPE/biomass mixture of 50/50 wt % (c) and pure HDPE (d).

3.3.4. Characterization of the coke deposited

In order to explain the effect of feeding composition on the evolution of conversion with time on stream, the coke deposited on the catalyst has been characterized by temperature programmed oxidation (TPO) and transmission electron microscopy (TEM) images. Figure 7 shows the TPO profiles of deactivated catalyst for three feedings: pure biomass, a mixture of HDPE/biomass of 50/50 wt % and pure HDPE. In the valorization of pure biomass, a main peak at around 600 ºC is observed, which

corresponds to a polyaromatic and structured coke, with a small shoulder at around 425 ºC related to coke whose combustion is activated by the Ni metallic sites. This coke can be related to the carbon whiskers reported by Trane-Restrup and Jensen [2] in the steam reforming of furfural and guaiacol at 600 ºC. On the other hand, in the steam reforming of the pyrolysis products of pure HDPE, a main peak at 580 ºC with a shoulder at 450 ºC was observed. The main peak corresponds to a structured and filamentous coke similar to that obtained by Wu and Williams [62] and Acomb et al. [63] in the reforming of polypropylene (PP), as it could be observed in TEM images which will be discussed later. The slight difference of maximum temperature (605 ºC for these authors) can be attributed to the higher porosity of the catalyst used by them, which complicates the combustion of the coke fraction which blocks the pores of the catalyst. The peaks for the mixture of biomass and HDPE are between the TPO profiles obtained for pure biomass and HDPE.

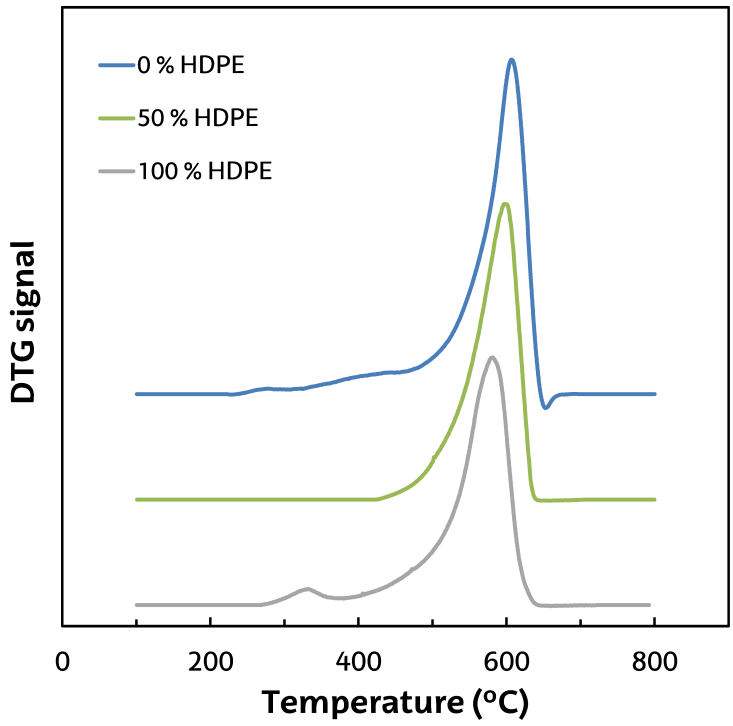

448 **Figure 7.** Comparison of TPO profiles of coke deposited in the catalyst for pure
449 biomass, HDPE/biomass mixture of 50/50 wt % and pure HDPE valorization.

450 Figure 8 shows TEM images of the deactivated catalyst for different feedings: pure
451 biomass (a), HDPE content in the feed of 25 wt % (b), 50 wt % (c), 75 wt % (d) and
452 pure HDPE (e). As observed, different structure and nature of the coke can be
453 distinguished, which is a consequence of the different composition of the volatiles fed
454 into the reforming step. In the images, Ni active sites can be identified as darker areas
455 and Figure 8a shows that the coke deposited is mainly non-structured for pure biomass
456 valorization, covering completely the Ni crystals (encapsulating coke). The presence of
457 amorphous and non-structured coke has also been observed in the catalytic steam
458 reforming of methane [64] different hydrocarbons [62,65] and oxygenated compounds
459 [2,66]. The high combustion temperature of this coke observed in TPO profile (600 ºC)
460 shows that it is a very condensed coke.

461 However, the structure of the coke changes when HDPE is co-fed, with its nature being
462 more filamentous as HDPE content in the feed is increased. This nature of filamentous
463 coke has been observed previously in the reforming of polyolefins pyrolysis products
464 [62,63].

465 Consequently, the faster deactivation observed for biomass and the attenuation of the
466 deactivation when HDPE is co-fed can be attributed to the different nature of the coke.
467 The amorphous coke formed in the reforming of oxygenated compounds derived from
468 biomass pyrolysis encapsulates the Ni centres, causing fast deactivation of the catalyst,
469 whereas the structured and filamentous coke formed mainly in the reforming of
470 hydrocarbons derived from HDPE pyrolysis do not block the Ni active centres, although
471 its progressive deposition complicates the gas flow of the reactants into Ni particles

472 [65,67]. This interpretation of the deactivation results is consistent with the fast
473 deactivation of the catalyst in the reforming of oxygenated compounds (DME, ethanol
474 and bio-oil), attributed to the encapsulation of Ni centres by the amorphous coke formed
475 by condensation of intermediate oxygenates [8,66,68,69]. The deactivation is lower in
476 the reforming of hydrocarbons produced in the pyrolysis of polyolefins, where the coke
477 is mainly structured [62,63].

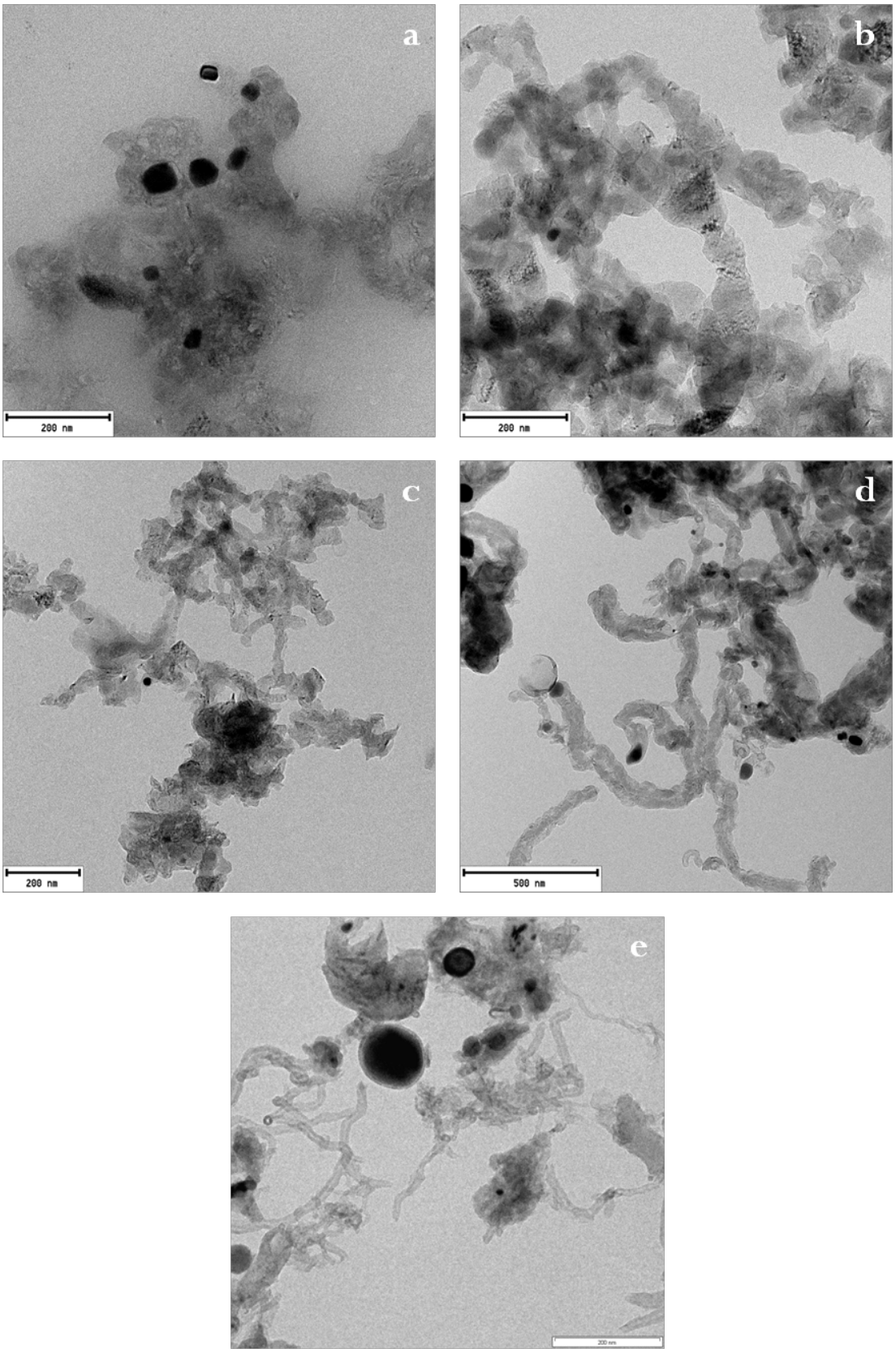

478

Figure 8. TEM images of the coke deposited on the catalyst for valorization of pure biomass (a), HDPE content in the feed of 25 wt % (b), 50 wt % (c), 75 wt % (d) and pure HDPE (e).

Conclusions

The continuous process of pyrolysis at 500 ºC in a CSBR followed by steam reforming at 700 ºC in a fluidised bed reactor has shown an excellent performance in the treatment of HDPE, biomass and their mixtures. The joint valorisation of both feedstocks has shown to be an interesting strategy as it increases the flexibility of the process and improves the process yields. In fact, the increase of the plastic content in the feed enhanced both the gas production and hydrogen production, increasing lineally the hydrogen production with HDPE content in the feed, from 10.9 g per 100 g of feed for pure biomass to 37.3 g for HDPE.

The composition of the feeding has a significant effect over the catalyst deactivation in the reforming step. Biomass processing causes a much faster deactivation rate, with this result being especially relevant as the effective space time (referred to mass of carbon reformed) is around 2.5 times higher than that used with HDPE. Thus, after 120 min of continuous operation the conversion dropped from total conversion to approximately 90 and 60 % for pure HDPE and pure biomass, respectively. Consequently, the co-feeding of HDPE to biomass is a suitable strategy to attenuate the catalyst deactivation. These results are explained by the different nature of coke deposited on the catalyst, with the amorphous coke being the main deactivating one, which is the main type of coke in biomass valorization. The feeding of HDPE gives ways to the formation of a structured and filamentous coke, whose presence has lower impact on catalyst activity.

Acknowledgments

503 This work was carried out with financial support from the Ministry of Economy and
504 Competitiveness of the Spanish Government (CTQ2013-45105-R and CTQ2015-69436-
505 R), the EDRF funds, the Basque Government (IT748-13) and the University of the
506 Basque Country (UFI 11/39).

507 **References**

508 [1] Acar C, Dincer I Comparative assessment of hydrogen production methods from renewable
509 and non-renewable sources. Int J Hydrogen Energy 2014;39:1-12.
510 doi:10.1016/j.ijhydene.2013.10.060.

511 [2] Trane-Restrup R, Jensen AD Steam reforming of cyclic model compounds of bio-oil over Ni-
512 based catalysts: Product distribution and carbon formation. Appl Catal B Environ
513 2015;165:117-27. doi:10.1016/j.apcatb.2014.09.026.

514 [3] Schmid JC, Wolfesberger U, Koppatz S, Pfeifer C, Hofbauer H Variation of feedstock in a
515 dual fluidized bed steam gasifier-influence on product gas, tar content, and composition.
516 Environmental Progress and Sustainable Energy 2012;31:205-15.

517 [4] Zhou C, Rosén C, Engvall K Biomass oxygen/steam gasification in a pressurized bubbling
518 fluidized bed: Agglomeration behavior. Appl Energy 2016;172:230-50.
519 doi:10.1016/j.apenergy.2016.03.106.

520 [5] Erkiaga A, Lopez G, Amutio M, Bilbao J, Olazar M Steam gasification of biomass in a conical
521 spouted bed reactor with olivine and g-alumina as primary catalysts. Fuel Process Technol
522 2013;116:292-9.

523 [6] Miccio F, Piriou B, Ruoppolo G, Chirone R Biomass gasification in a catalytic fluidized reactor
524 with beds of different materials. Chem Eng J 2009;154:369-74.

525 [7] Bimbela F, Oliva M, Ruiz J, García L, Arauzo J Hydrogen production via catalytic steam
526 reforming of the aqueous fraction of bio-oil using nickel-based coprecipitated catalysts. Int J
527 Hydrogen Energy 2013;38:14476-87. doi:http://dx.doi.org/10.1016/j.ijhydene.2013.09.038.

528 [8] Remiro A, Valle B, Aguayo AT, Bilbao J, Gayubo AG Steam reforming of raw bio-oil in a
529 fluidized bed reactor with prior separation of pyrolytic lignin. Energy and Fuels 2013;27:7549-
530 59.

531 [9] Kechagiopoulos PN, Voutetakis SS, Lemonidou AA, Vasalos IA Hydrogen production via
532 reforming of the aqueous phase of bio-oil over Ni/olivine catalysts in a spouted bed reactor.
533 Industrial and Engineering Chemistry Research 2009;48:1400-8.

534 [10] Kan T, Xiong J, Li X, et al. High efficient production of hydrogen from crude bio-oil via an
535 integrative process between gasification and current-enhanced catalytic steam reforming.
536 International Journal of Hydrogen Energy 2010;35:518-32.

[11] Tsuboi Y, Ito S, Takafuji M, Ohara H, Fujimori T Development of a regenerative reformer for tar-free syngas production in a steam gasification process. Appl Energy . doi:http://dx.doi.org/10.1016/j.apenergy.2015.12.110.

[12] Abdoulmoumine N, Adhikari S, Kulkarni A, Chattanathan S A review on biomass gasification syngas cleanup. Appl Energy 2015;155:294-307. doi:10.1016/j.apenergy.2015.05.095.

[13] Czernik S, French R Distributed production of hydrogen by auto-thermal reforming of fast pyrolysis bio-oil. Int J Hydrogen Energy 2014;39:744-50. doi:http://dx.doi.org/10.1016/j.ijhydene.2013.10.134.

[14] Lehto J., Oasmaa A., Solantausta Y., Kytö M., Chiaramonti D. Review of fuel oil quality and combustion of fast pyrolysis bio-oils from lignocellulosic biomass. Appl Energy 2014;116:178-90. doi:10.1016/j.apenergy.2013.11.040.

[15] Xiao X, Cao J, Meng X, et al. Synthesis gas production from catalytic gasification of waste biomass using nickel-loaded brown coal char. Fuel 2013;103:135-40. doi:10.1016/j.fuel.2011.06.077.

[16] Ma Z, Zhang S-, Xie D-, Yan Y- A novel integrated process for hydrogen production from biomass. Int J Hydrogen Energy 2014;39:1274-9. doi:10.1016/j.ijhydene.2013.10.146.

[17] Arregi A, Lopez G, Amutio M, Barbarias I, Bilbao J, Olazar M Hydrogen production from biomass by continuous fast pyrolysis and in-line steam reforming. RSC Adv 2016;6:25975-85. doi:10.1039/C6RA01657J.

[18] Koike M, Ishikawa C, Li D, Wang L, Nakagawa Y, Tomishige K Catalytic performance of manganese-promoted nickel catalysts for the steam reforming of tar from biomass pyrolysis to synthesis gas. Fuel 2013;103:122-9.

[19] Chen F, Wu C, Dong L, Vassallo A, Williams PT, Huang J Characteristics and catalytic properties of Ni/CaAlOx catalyst for hydrogen-enriched syngas production from pyrolysis-steam reforming of biomass sawdust. Applied Catalysis B: Environmental 2016;183:168-75. doi:http://dx.doi.org/10.1016/j.apcatb.2015.10.028.

[20] Alvarez J, Kumagai S, Wu C, Yoshioka T, Bilbao J, Olazar M Hydrogen production from biomass and plastic mixtures by pyrolysis-gasification. International Journal of Hydrogen Energy 2014;39:10883-91.

[21] Wilk V, Hofbauer H Co-gasification of plastics and biomass in a dual fluidized-bed steam gasifier: Possible interactions of fuels. Energy and Fuels 2013;27:3261-73.

[22] Pinto F, Franco C, Andre RN, Miranda M, Gulyurtlu I, Cabrita I Co-gasification study of biomass mixed with plastic wastes. Fuel 2002;81:291-7.

[23] Lopez G, Erkiaga A, Amutio M, Bilbao J, Olazar M Effect of polyethylene co-feeding in the steam gasification of biomass in a conical spouted bed reactor. Fuel 2015;153:393-401. doi:http://dx.doi.org/10.1016/j.fuel.2015.03.006.

574 [24] Ruoppolo G, Ammendola P, Chirone R, Miccio F H 2-rich syngas production by fluidized
575 bed gasification of biomass and plastic fuel. Waste Manage 2012;32:724-32.

576 [25] Wong SL, Ngadi N, Abdullah TAT, Inuwa IM Current state and future prospects of plastic
577 waste as source of fuel: A review. Renewable and Sustainable Energy Reviews 2015;50:1167-
578 80. doi:http://dx.doi.org/10.1016/j.rser.2015.04.063.

579 [26] Kunwar B, Cheng HN, Chandrashekaran SR, Sharma BK Plastics to fuel: a review.
580 Renewable Sustainable Energy Rev 2016;54:421-8. doi:10.1016/j.rser.2015.10.015.

581 [27] Anuar Sharuddin SD, Abnisa F, Wan Daud WMA, Aroua MK A review on pyrolysis of plastic
582 wastes. Energy Convers Manage 2016;115:308-26. doi:10.1016/j.enconman.2016.02.037.

583 [28] Kumagai S, Alvarez J, Blanco PH, et al. Novel Ni-Mg-Al-Ca catalyst for enhanced hydrogen
584 production for the pyrolysis-gasification of a biomass/plastic mixture. J Anal Appl Pyrolysis
585 2015;113:15-21. doi:10.1016/j.jaap.2014.09.012.

586 [29] Amutio M, Lopez G, Artetxe M, Elordi G, Olazar M, Bilbao J Influence of temperature on
587 biomass pyrolysis in a conical spouted bed reactor. Resources, Conservation and Recycling
588 2012;59:23-31.

589 [30] Elordi G, Olazar M, Lopez G, Artetxe M, Bilbao J Product Yields and Compositions in the
590 Continuous Pyrolysis of High-Density Polyethylene in a Conical Spouted Bed Reactor. Ind Eng
591 Chem Res 2011;50:6650-9.

592 [31] Lan P, Xu Q, Zhou M, Lan L, Zhang S, Yan Y Catalytic steam reforming of fast pyrolysis bio-
593 oil in fixed bed and fluidized bed reactors. Chemical Engineering and Technology
594 2010;33:2021-8.

595 [32] Tsuji T, Hatayama A Gasification of waste plastics by steam reforming in a fluidized bed.
596 Journal of Material Cycles and Waste Management 2009;11:144-7.

597 [33] Barbarias I, Lopez G, Alvarez J, et al. A sequential process for hydrogen production based
598 on continuous HDPE fast pyrolysis and in-line steam reforming. Chem Eng J 2016;296:191-8.
599 doi:http://dx.doi.org/10.1016/j.cej.2016.03.091.

600 [34] Erkiaga A, Lopez G, Barbarias I, et al. HDPE pyrolysis-steam reforming in a tandem spouted
601 bed-fixed bed reactor for H2 production. J Anal Appl Pyrolysis 2015;116:34-41.
602 doi:http://dx.doi.org/10.1016/j.jaap.2015.10.010.

603 [35] Lopez G, Erkiaga A, Artetxe M, Amutio M, Bilbao J, Olazar M Hydrogen Production by High
604 Density Polyethylene Steam Gasification and In-Line Volatile Reforming. Ind Eng Chem Res
605 2015;54:9536-44. doi:10.1021/acs.iecr.5b02413.

606 [36] Alvarez J, Amutio M, Lopez G, Barbarias I, Bilbao J, Olazar M Sewage sludge valorization by
607 flash pyrolysis in a conical spouted bed reactor. Chem Eng J 2015;273:173-83.
608 doi:http://dx.doi.org/10.1016/j.cej.2015.03.047.

609 [37] Erkiaga A, Lopez G, Amutio M, Bilbao J, Olazar M Syngas from steam gasification of
610 polyethylene in a conical spouted bed reactor. Fuel 2013;109:461-9.

611 [38] Artetxe M, Lopez G, Amutio M, Elordi G, Bilbao J, Olazar M Cracking of high density
612 polyethylene pyrolysis waxes on HZSM-5 catalysts of different acidity. Industrial and
613 Engineering Chemistry Research 2013;52:10637-45.

614 [39] Lopez G, Olazar M, Aguado R, Bilbao J Continuous pyrolysis of waste tyres in a conical
615 spouted bed reactor. Fuel 2010;89:1946-52.

616 [40] Lopez G, Olazar M, Amutio M, Aguado R, Bilbao J Influence of Tire Formulation on the
617 Products of Continuous Pyrolysis in a Conical Spouted Bed Reactor. Energy Fuels
618 2009;23:5423-31.

619 [41] Mellin P, Kantarelis E, Zhou C, Yang W Simulation of bed dynamics and primary products
620 from fast pyrolysis of biomass: Steam compared to nitrogen as a fluidizing agent. Ind Eng Chem
621 Res 2014;53:12129-42. doi:10.1021/ie501996v.

622 [42] Kaminsky W, Schlesselmann B, Simon C Olefins from polyolefins and mixed plastics by
623 pyrolysis. J Anal Appl Pyrolysis 1995;32:19-27.

624 [43] Alvarez J, Lopez G, Amutio M, Bilbao J, Olazar M Upgrading the rice husk char obtained by
625 flash pyrolysis for the production of amorphous silica and high quality activated carbon.
626 Bioresour Technol 2014;170:132-7.

627 [44] Al Bahri M, Calvo L, Gilarranz MA, Rodriguez JJ Activated carbon from grape seeds upon
628 chemical activation with phosphoric acid: Application to the adsorption of diuron from water.
629 Chem Eng J 2012;203:348-56. doi:10.1016/j.cej.2012.07.053.

630 [45] Shen Y, Zhao P, Shao Q, Takahashi F, Yoshikawa K In situ catalytic conversion of tar using
631 rice husk char/ash supported nickel-iron catalysts for biomass pyrolytic gasification combined
632 with the mixing-simulation in fluidized-bed gasifier. Appl Energy 2015;160:808-19.
633 doi:10.1016/j.apenergy.2014.10.074.

634 [46] Zazo JA, Bedia J, Fierro CM, Pliego G, Casas JA, Rodriguez JJ Highly stable Fe on activated
635 carbon catalysts for CWPO upon FeCl 3 activation of lignin from black liquors. Catal Today
636 2012;187:115-21. doi:10.1016/j.cattod.2011.10.003.

637 [47] Monlau F, Francavilla M, Sambusiti C, et al. Toward a functional integration of anaerobic
638 digestion and pyrolysis for a sustainable resource management. Comparison between solid-
639 digestate and its derived pyrochar as soil amendment. Appl Energy 2016;169:652-62.
640 doi:10.1016/j.apenergy.2016.02.084.

641 [48] Artetxe M, Lopez G, Elordi G, Amutio M, Bilbao J, Olazar M Production of Light Olefins
642 from Polyethylene in a Two-Step Process: Pyrolysis in a Conical Spouted Bed and Downstream
643 High-Temperature Thermal Cracking. Ind Eng Chem Res 2012;51:13915-23.

644 [49] Czernik S, Evans R, French R Hydrogen from biomass-production by steam reforming of
645 biomass pyrolysis oil. Catalysis Today 2007;129:265-8.

646 [50] Bhattacharya P, Steele PH, Hassan EBM, Mitchell B, Ingram L, Pittman Jr. CU Wood/plastic
647 copyrolysis in an auger reactor: Chemical and physical analysis of the products. Fuel
648 2009;88:1251-60. doi:10.1016/j.fuel.2009.01.009.

649 [51] Xue Y, Zhou S, Brown RC, Kelkar A, Bai X Fast pyrolysis of biomass and waste plastic in a
650 fluidized bed reactor. Fuel 2015;156:40-6. doi:10.1016/j.fuel.2015.04.033.

651 [52] Xiao X, Meng X, Le DD, Takarada T Two-stage steam gasification of waste biomass in
652 fluidized bed at low temperature: Parametric investigations and performance optimization.
653 Bioresour Technol 2011;102:1975-81.

654 [53] Czernik S, French RJ Production of hydrogen from plastics by pyrolysis and catalytic steam
655 reform. Energy and Fuels 2006;20:754-8.

656 [54] Ahmed II, Nipattummakul N, Gupta AK Characteristics of syngas from co-gasification of
657 polyethylene and woodchips. Applied Energy 2011;88:165-74.

658 [55] Koppatz S, Pfeifer C, Hofbauer H Comparison of the performance behaviour of silica sand
659 and olivine in a dual fluidised bed reactor system for steam gasification of biomass at pilot
660 plant scale. Chem Eng J 2011;175:468-83.

661 [56] Michel R, Rapagn S, Di Marcello M, et al. Catalytic steam gasification of Miscanthus X
662 giganteus in fluidised bed reactor on olivine based catalysts. Fuel Process Technol
663 2011;92:1169-77.

664 [57] He M, Xiao B, Hu Z, Liu S, Guo X, Luo S Syngas production from catalytic gasification of
665 waste polyethylene: Influence of temperature on gas yield and composition. International
666 Journal of Hydrogen Energy 2009;34:1342-8.

667 [58] Narobe M, Golob J, Klinar D, Francetic V, Likozar B Co-gasification of biomass and plastics:
668 Pyrolysis kinetics studies, experiments on 100kW dual fluidized bed pilot plant and
669 development of thermodynamic equilibrium model and balances. Bioresour Technol
670 2014;162:21-9. doi:10.1016/j.biortech.2014.03.121.

671 [59] Trane R, Dahl S, Skjoth-Rasmussen MS, Jensen AD Catalytic steam reforming of bio-oil.
672 International Journal of Hydrogen Energy 2012;37:6447-72.

673 [60] Rioche C, Kulkarni S, Meunier FC, Breen JP, Burch R Steam reforming of model compounds
674 and fast pyrolysis bio-oil on supported noble metal catalysts. Applied Catalysis B:
675 Environmental 2005;61:130-9. doi:http://dx.doi.org/10.1016/j.apcatb.2005.04.015.

676 [61] Lemonidou AA, Kechagiopoulos P, Heracleous E, Voutetakis S Steam Reforming of Bio-oils
677 to Hydrogen. The Role of Catal for the Sustain Prod of Bio-Fuels and Bio-Chem 2013:467-93.
678 doi:10.1016/B978-0-444-56330-9.00014-0.

679 [62] Wu C, Williams PT Investigation of coke formation on Ni-Mg-Al catalyst for hydrogen
680 production from the catalytic steam pyrolysis-gasification of polypropylene. Applied Catalysis
681 B: Environmental 2010;96:198-207.

682 [63] Acomb JC, Wu C, Williams PT Control of steam input to the pyrolysis-gasification of waste
683 plastics for improved production of hydrogen or carbon nanotubes. Applied Catalysis B:
684 Environmental 2014;147:571-84.

685 [64] Angeli SD, Pilitsis FG, Lemonidou AA Methane steam reforming at low temperature: Effect
686 of light alkanes' presence on coke formation. Catal Today 2015:119-28.
687 doi:10.1016/j.cattod.2014.05.043.

688 [65] Barbarias I, Lopez G, Amutio M, et al.
Steam reforming of plastic pyrolysis model
689 hydrocarbons and catalyst deactivation. Chem Eng J 2016;Submitted for publication.
690 doi:10.1016/j.cej.2016.03.091.

691 [66] Montero C, Ochoa A, Castaño P, Bilbao J, Gayubo AG Monitoring Ni^0 and coke evolution
692 during the deactivation of a Ni/La2O3-aAl2O3 catalyst in ethanol steam reforming in a fluidized
693 bed. J Catal 2015;331:181-92. doi:10.1016/j.jcat.2015.08.005.

694 [67] Latorre N, Cazaña F, Martínez-Hansen V, Royo C, Romeo E, Monzón A Ni-Co-Mg-Al
695 catalysts for hydrogen and carbonaceous nanomaterials production by CCVD of methane. Catal
696 Today 2011;172:143-51. doi:10.1016/j.cattod.2011.02.038.

697 [68] Vicente J, Ereña J, Montero C, Azkoiti MJ, Bilbao J, Gayubo AG Reaction pathway for
698 ethanol steam reforming on a Ni/SiO2 catalyst including coke formation. Int J Hydrogen Energy
699 2014;39:18820-34.

700 [69] Vicente J, Montero C, Ereña J, Azkoiti MJ, Bilbao J, Gayubo AG Coke deactivation of Ni and
701 Co catalysts in ethanol steam reforming at mild temperatures in a fluidized bed reactor. Int J
702 Hydrogen Energy 2014;39:12586-96.

703